A Kinetically Defined Na^+/H^+ Antiporter within a Mathematical Model of the Rat Proximal Tubule

ALAN M. WEINSTEIN

From the Department of Physiology and Biophysics, Cornell University Medical College, New York, New York 10021

ABSTRACT The luminal membrane antiporter of the proximal tubule has been represented using the kinetic formulation of E. Heinz (1978. Mechanics and Engergetics of Biological Transport. Springer-Verlag, Berlin) with the assumption of equilibrium binding and 1:1 stoichiometry. Competitive binding and transport of NH_4^+ is included within this model. Ion affinities and permeation velocities were selected in a least-squares fit to the kinetic parameters determined experimentally in renal membrane vesicles (Aronson, P. S., M. A. Suhm, and J. Nee. 1983. *Journal of Biological Chemistry.* 258:6767–6771). The modifier role of internal H^+ to enhance transport beyond the expected kinetics (Aronson, P. S., J. Nee, and M. A. Suhm. 1982. *Nature.* 299:161–163) is represented as a velocity effect of H^+ binding to a single site. This kinetic formulation of the Na^+/H^+ antiporter was incorporated within a model of the rat proximal tubule (Weinstein, A. M. 1994. *American Journal of Physiology.* 267:F237–F248) as a replacement for the representation by linear nonequilibrium thermodynamics (NET). The membrane density of the antiporter was selected to yield agreement with the rate of tubular Na^+ reabsorption. Simulation of 0.5 cm of tubule predicts that the activity of the Na^+/H^+ antiporter is the most important force for active secretion of ammonia. Model calculations of metabolic acid-base disturbances are performed and comparison is made among antiporter representations (kinetic model, kinetic model without internal modifier, and NET formulation). It is found that the ability to sharply turn off Na^+/H^+ exchange in cellular alkalosis substantially eliminates the cell volume increase associated with high HCO_3^- conditions. In the tubule model, diminished Na^+/H^+ exchange in alkalosis blunts the axial decrease in luminal HCO_3^- and thus diminishes paracellular reabsorption of Cl^-. In this way, the kinetics of the Na^+/H^+ antiporter could act to enhance distal delivery of Na^+, Cl^-, and HCO_3^- in acute metabolic alkalosis.

INTRODUCTION

Sodium transport by proximal tubule must be understood in terms of the function of the luminal membrane Na^+/H^+ antiporter. This transporter mediates the one-for-

Address correspondence to Dr. Alan M. Weinstein, Department of Physiology and Biophysics, Cornell University Medical College, 1300 York Avenue, New York, NY 10021.

J. GEN. PHYSIOL. © The Rockefeller University Press · 0022-1295/95/05/0617/25 $2.00
Volume 105 May 1995 617–641

one exchange of Na^+ for H^+ (Murer, Hopfer, and Kinne, 1976; Kinsella and Aronson, 1980, 1982) and its activity is enhanced by cytosolic acidosis (Aronson, Nee, and Suhm, 1982). Beyond mediating most of $NaHCO_3$ reabsorption, it is also likely that the antiporter is responsible for the bulk of proximal NaCl reabsorption, functioning in parallel with Cl^-/anion exchange (Lucci and Warnock, 1979; Preisig and Rector, 1988). This, along with the fact that luminal entry is rate limiting for transcellular sodium flux, renders the antiporter ideally suited as a regulatory site for proximal reabsorption. Indeed, the Na^+/H^+ antiporter is the target of several hormone systems that modify proximal reabsorption: it is enhanced by angiotensin II (Harris and Navar, 1985; Liu and Cogan, 1988; Cogan 1990) and by catecholamines (Bello-Reuss, 1980; Weinman, Sansom, Knight, and Senekjian, 1982; Nord, Goldfarb, Mikhail, Moradeshagi, Hafezi, Vaystub, Cragoe, and Fine, 1987) and inhibited by dopamine (Felder, Campbell, Albrecht, and Jose, 1990). The Na^+/H^+ antiporter also appears to be a key mediator of perfusion-absorption balance, i.e., the flow-dependent component of glomerulotubular balance. Increases in luminal perfusion are associated with sharp increases in proximal HCO_3^- reabsorption (Chan, Biagi, and Giebisch, 1982; Alpern, Cogan, and Rector, 1983) and this has been shown to be a direct enhancement of Na^+/H^+ exchange activity (Preisig, 1992).

The transport kinetics of the proximal tubule luminal membrane Na^+/H^+ antiporter have been studied intensively (Aronson, 1985; Grinstein and Rothstein, 1986; Montrose and Murer, 1988). Examination of isolated membrane preparations revealed a transport site that bound a single Na^+ (Warnock, Reenstra, and Yee, 1982) with an affinity roughly one tenth that of the external Na^+ concentration and with competitive binding by H^+ or NH_4^+ (Kinsella and Aronson, 1981; Aronson, Suhm, and Nee, 1983). Studies of the antiporter at lower temperatures indicated that Na^+ and H^+ extrusion occurred in a sequential (ping pong) fashion with H^+ transport likely to be the rate-limiting step (Otsu, Kinsella, Sacktor, and Froehlich, 1989; Otsu, Kinsella, Koh, and Froelich, 1992). The effect of intracellular pH is more complex, with cytosolic alkalosis shutting off Na^+/H^+ exchange more sharply than a simple substrate depletion effect (Aronson et al., 1983). Cytosolic pH appears to have little impact on the Na^+ affinity of the antiporter (Kinsella, Cujdik, and Sacktor, 1986), but rather modifies the turnover rate (Otsu et al., 1989). When intact proximal tubule cells were examined, there were no inconsistencies observed with the kinetic parameters established in vesicle preparations (Nord et al., 1986). More recently, Na^+/H^+ antiporters have been recognized as a family of transport proteins, with the proximal tubule luminal membrane exchanger identified as NHE-3. The gene for NHE-3 has been cloned and sequenced (Tse, Brant, Walker, Pouyssegur, and Donowitz, 1992; Orlowski, Kandasamy, and Shull, 1991) and the product identified immunocytochemically in the brush border membrane (Beimesderfer, Pizzonia, Abu-Alfa, Exner, Reilly, Igarashi, and Aronson, 1993). Again, kinetic studies of the expressed NHE-3 have confirmed the properties noted a decade earlier in the membrane preparations (Tse, Levine, Yun, Brant, Pouyssegur, Montrose, and Donowitz, 1993; Orlowski, 1993).

With the Na^+/H^+ antiporter, the primary regulatory site for proximal sodium reabsorption, flux changes will of necessity impact on cell pH, on cell volume, and on proximal ammonia transport. Thus, the antiporter is situated in a setting of sufficient

complexity that a mathematical model is a natural tool for delineating the impact of transport parameters on tissue function. Although a number of computer simulations of proximal tubule have been developed, only two have attempted to represent the kinetics of the Na^+/H^+ antiporter. The first attempt was that of Verkman and Alpern (1987) whose epithelial model focused on the interplay of the luminal antiporter and the peritubular Na^+–$3HCO_3^-$ cotransporter in the transient response to perturbations of bathing solution composition. More recently, Thomas and Dagher (1994) modeled a proximal tubule segment in order to investigate how transporter kinetics relate to flow dependence of bicarbonate reabsorption.

Models from this laboratory have heretofore relied on linear nonequilibrium thermodynamics to represent flux through the Na^+/H^+ antiporter. With this formulation, flux is a linear function of the transmembrane electrochemical potential differences of Na^+ and H^+, with a single constant transport coefficient. Once this coefficient is determined (by the overall rate of Na^+ reabsorption) the kinetics are completely defined. In the present work, the approach of Heinz (1978) is used to fashion a kinetic model for the Na^+/H^+ antiporter. This model contains four parameters (Na^+ and H^+ affinity, the ratio of Na^+:H^+ permeation rates, and transporter density) and these are fit to the data of Aronson et al. (1983). Modification (with one additional parameter) is introduced to accommodate the observation of the internal H^+ modifier site (Aronson et al., 1982). This more sophisticated transporter is then incorporated into preexisting models of proximal epithelium and tubule (Weinstein, 1994). With these models, we illustrate the impact of the internal pH dependence for Na^+/H^+ exchange, on both cell volume homeostasis and overall tubule transport in metabolic alkalosis.

MODEL EQUATIONS

The approach of Heinz (1978) for an electroneutral antiporter is depicted in Fig. 1 in which a single transport site, X, may be oriented toward the external (X') or internal (X'') membrane face. The analysis of Heinz (1978) is extended with the inclusion of three solute species (A, B, and C) which will be thought of as Na^+, H^+, and NH_4^+, and which bind competitively to the transport site. The external complexes, AX', BX', CX', and the internal complexes AX'', BX'', CX'', may traverse the membrane according to their respective permeation coefficients, P_a, P_b, and P_c. Following Heinz (1978), it will be assumed that (a) ion binding is rapid relative to membrane translocation, so that the proportion of complexed to free carrier may be represented by equilibrium constants, and (b) the affinity of ion binding is symmetric, so that the equilibrium constants for inner and outer membrane faces are equal:

$$K_a = \frac{a' \cdot x'}{ax'} = \frac{a'' \cdot x''}{ax''} \qquad K_b = \frac{b' \cdot x'}{bx'} = \frac{b'' \cdot x''}{bx''} \qquad K_c = \frac{c' \cdot x'}{cx'} = \frac{c'' \cdot x''}{cx''} \tag{1}$$

In Eq. 1, the lower case variables (e.g., a' or ax') denote the concentration or density of the associated upper case species (A' or AX'). Relaxation of the equilibrium assumption yields models of considerably greater flexibility (Sanders, Hansen, Gradmann, and Slayman, 1984) but the complexity of such an approach appears not

to be required for the considerations of this work. Similarly, there appear to be no experimental data that address the symmetry of substrate affinity of the Na^+/H^+ exchanger. Consequently, the simplest assumption, namely symmetric binding, is used in this model. Once the binding affinity is asymmetric, then the permeation coefficients are also asymmetric (i.e., distinct forward and reverse constants). With symmetry for the equilibrium binding constants, energetics of a passive carrier require equality of the forward and reverse rate constants for carrier translocation, namely a single permeation coefficient (P_a, P_b, or P_c).

Corresponding to the two unknowns, x' and x'', are the model equations for conservation of total carrier

$$x' + ax' + bx' + cx' + x'' + ax'' + bx'' + cx'' = x_T \tag{2}$$

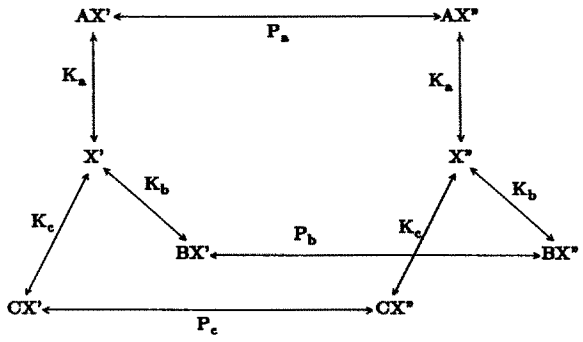

FIGURE 1. Schematic representation of the Na^+/H^+ antiporter. The carrier may either be empty, X, or bound to one of three ions, Na^+, H^+, or NH_4^+, designated XA, XB, or XC. Binding is rapid, and defined by equilibrium constants K_a, K_b, and K_c. The carrier or carrier-ion complex may face either the external (') or internal (") membrane surface. Translocation of the loaded carrier occurs according to rate coefficients P_a, P_b, and P_c. There is no translocation of empty carrier.

and for zero net flux of carrier

$$P_a ax' + P_b bx' + P_c cx' = P_a ax'' + P_b bx'' + P_c cx''. \tag{3}$$

In Eq. 3, the left- and right-hand sides represent the unidirectional inward and outward flxues of the carrier. Of note, there is no flux of unloaded carrier (slippage), corresponding to a strict 1:1 stoichiometry for a two-ion system. If one denotes normalized concentrations for both internal and external faces by

$$\alpha = \frac{a}{K_a} \qquad \beta = \frac{b}{K_b} \qquad \gamma = \frac{c}{K_c} \tag{4}$$

then using the equilibrium (Eq. 1), Eqs. 2 and 3 may be rewritten

$$x'(1 + \alpha' + \beta' + \gamma') + x''(1 + \alpha'' + \beta'' + \gamma'') = x_T \tag{5}$$

$$x'(P_a\alpha' + P_b\beta' + P_c\gamma') - x''(P_a\alpha'' + P_b\beta'' + P_c\gamma'') = 0. \tag{6}$$

When this linear system is solved for x' and x'', the individual transmembrane solute fluxes are

$$J_a = P_a(ax' - ax'') = \frac{P_aP_bx_T}{\Sigma}(\alpha'\beta'' - \alpha''\beta') + \frac{P_aP_cx_T}{\Sigma}(\alpha'\gamma'' - \alpha''\gamma') \tag{7}$$

$$J_b = P_b(bx' - bx'') = \frac{P_aP_bx_T}{\Sigma}(\beta'\alpha'' - \beta''\alpha') + \frac{P_bP_cx_T}{\Sigma}(\beta'\gamma'' - \beta''\gamma') \tag{8}$$

$$J_c = P_c(cx' - cx'') = \frac{P_aP_cx_T}{\Sigma}(\gamma'\alpha'' - \gamma''\alpha') + \frac{P_bP_cx_T}{\Sigma}(\gamma'\beta'' - \gamma''\beta') \tag{9}$$

where

$$\Sigma = (1 + \alpha' + \beta' + \gamma')(P_a\alpha'' + P_b\beta'' + P_c\gamma'') + (1 + \alpha'' + \beta'' + \gamma'')(P_a\alpha' + P_b\beta' + P_c\gamma') \tag{10}$$

To render these equations into the form of linear nonequilibrium thermodynamics, one applies the approximation

$$\alpha'\beta'' - \alpha''\beta' \approx \left(\frac{\alpha'\beta'' + \alpha''\beta'}{2}\right)\left[\ln\left(\frac{\alpha'}{\alpha''}\right) - \ln\left(\frac{\beta'}{\beta''}\right)\right] = \frac{\overline{\alpha\beta}}{RT}(\mu_\alpha - \mu_\beta) \tag{11}$$

where $\mu_\alpha = RT\ln(\alpha'/\alpha'')$. Using similar formulas for the other differences one obtains the fluxes.

$$\begin{aligned}
J_a &\approx \frac{x_T}{RT\Sigma}[(P_aP_b\overline{\alpha\beta} + P_aP_c\overline{\alpha\gamma})\mu_\alpha - P_aP_b\overline{\alpha\beta}\mu_\beta - P_aP_c\overline{\alpha\gamma}\mu_\gamma] \\
J_b &\approx \frac{x_T}{RT\Sigma}[-P_aP_b\overline{\alpha\beta}\mu_\alpha + (P_aP_b\overline{\alpha\beta} + P_bP_c\overline{\beta\gamma})\mu_\beta - P_bP_c\overline{\beta\gamma}\mu_\gamma] \\
J_c &\approx \frac{x_T}{RT\Sigma}[-P_aP_c\overline{\alpha\gamma}\mu_\alpha - P_bP_c\overline{\beta\gamma}\mu_\beta + (P_aP_c\overline{\alpha\gamma} + P_bP_c\overline{\beta\gamma})\mu_\gamma]
\end{aligned} \tag{12}$$

It is clear from these expressions that the coupling of the three ion species via this single carrier is different from including both an Na^+/H^+ and Na^+/NH_4^+ antiporter, as had been done previously (Weinstein, 1994).

In the absence of NH_4^+($\gamma' = \gamma'' = 0$), the model equations display equal and opposite Na^+ and H^+ fluxes. Under the zero *trans* Na^+ condition frequently employed in the study of vesicle systems ($\alpha'' = 0$) the antiporter flux is

$$J_a = \frac{P_aP_bx_T}{\Sigma}\alpha'\beta'' = P_aP_bx_T\left[\frac{\alpha'\beta''}{\beta'P_b(1 + 2\beta'') + (1 + \alpha')P_b\beta'' + (1 + \beta'')P_a\alpha'}\right]. \tag{13}$$

This last formulation reveals the explicit inhibition by *cis* protons (β') with a half-maximal inhibition concentration

$$K_H = \frac{(1 + \alpha')\beta'' + (1 + \beta'')\alpha'(P_a/P_b)}{1 + 2\beta''} \tag{14}$$

Alternatively, one may write the reciprocal of Eq. 13 to determine the Na^+ concentration for half-maximal flux

$$\frac{1}{J_a} = \frac{1}{P_a P_b x_T \beta''}\left[\frac{P_b}{\alpha'}(\beta'' + 2\beta'\beta'' + \beta') + P_b\beta'' + P_a(1 + \beta'')\right] \tag{15}$$

so that

$$K_{Na} = \frac{\beta'' + 2\beta'\beta'' + \beta'}{\beta'' + (1 + \beta'')(P_a/P_b)}. \tag{16}$$

What should be noted in Eqs. 14 and 16, is that the Michaelis constants for Na^+ and H^+ depend upon both individual equilibrium binding constants of the model antiporter (K_a and K_b), but only the ratio of the permeation coefficients (P_a/P_b). In the selection of model parameters, these three parameters will be fit to vesicle data. The absolute permeation velocities will be determined from the desired rate of overall Na^+ reabsorption.

The one aspect of the model not included in the scheme of Fig. 1 is the internal modifier site. Clearly, one could enhance the turnover rate of the model antiporter by increases in P_a or P_b or by decreases in the equilibrium constants K_a or K_b or by some combination of these. As indicated above, Kinsella et al. (1986) could demonstrate no effect of cytosolic pH on K_{Na}. With reference to Eq. 16, such a constraint could be accommodated if P_a and P_b increased proportionally with cytosolic acidification. This could be interpreted as a decrease in the activation energy for conformational shifts between inside and outside-facing loaded carriers. To represent such a scheme, we consider a single internal site, Y, which can also exist as HY, with equilibrium binding constant, K_y. The density of the bound sites is

$$\frac{[HY]}{y_T} = \frac{[H]}{K_y + [H]} \tag{17}$$

where $y_T = [Y] + [HY]$ is the total carrier density, and it will be assumed that the permeation velocity of each species $P_i \sim (i = a,b,c)$ varies linearly with this density:

$$(P_i^m - P_i^0)\frac{[HY]}{y_T} = P_i - P_i^0 \tag{18}$$

where P_i^m and P_i^0 represent the maximal and minimal permeation velocities corresponding to fully bound or unbound modifier sites. Substitution of Eq. 17 into Eq. 18 yields

$$P_i = \frac{P_i^m[H] + P_i^0 K_y}{[H] + K_y} \tag{19}$$

so that the permeation velocity is a weighted average of the maximal and minimum values, with half-maximal velocity at $[H] = K_y$.

MODEL CALCULATIONS

The upper portion of Table I contains the equilibrium constants, K_i, and permeation velocities, P_i, for the model antiporter at internal pH 6.0. Aronson et al. (1983)

TABLE I

Na/H Antiporter Model Parameters

	At internal pH 6.0	
	K *mol/l*	$P_0 x_T$ *cm/s*
Na^+	0.030	1.60×10^{-5}
H^+	72.0×10^{-9}	0.48×10^{-5}
NH_4^+	0.027	1.60×10^{-5}

Internal modifier

$$P(i) = P_0(i)\frac{f^M C_I(H^+) + f^m K_I}{C_I(H^+) + K_I}$$

f^M	2.0
f^m	0.0
K_I (mol/liter)	1.0×10^{-6}

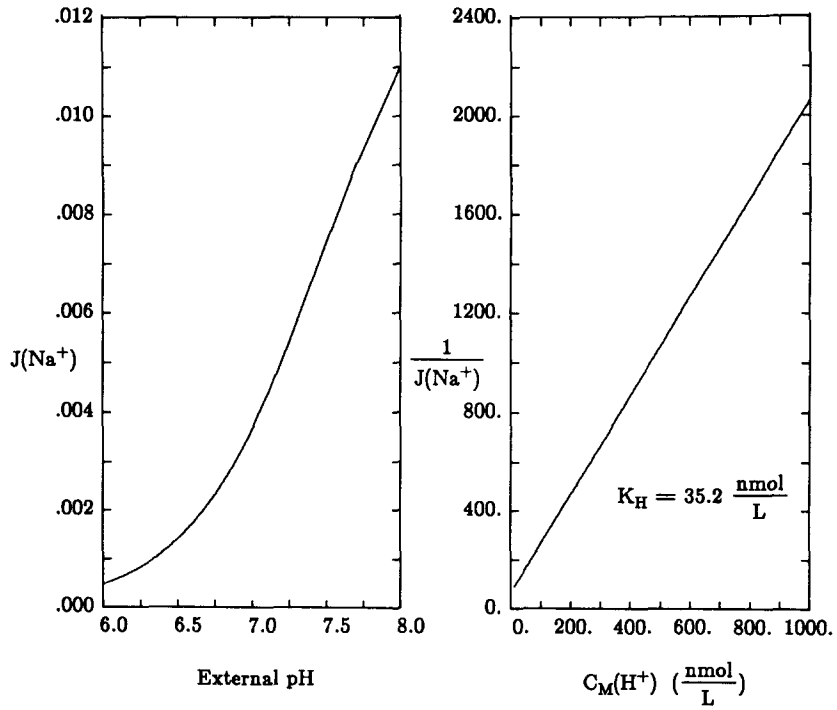

FIGURE 2. Effect of external pH on Na^+ influx. Model parameters are from Table I; internal pH 6.0, internal Na^+ = 0.0 mmol/liter, and external Na^+ = 0.1 mmol/liter. NH_4^+ is absent. (*Left*) Na^+ flux (relative to maximal zero *trans* flux) is plotted as a function of external pH. (*Right*) Reciprocal flux is plotted as a function of the external H^+ concentration.

determined that at this internal pH, the K_{Na} for zero *trans* Na^+ uptake was 54 mmol/liter at external pH 6.6 and 13 mmol/liter at external pH 7.5. They also noted that the apparent inhibitory Michaelis constant for external protons, K_H = 35 nmol/liter. Given these three observations, Eqs. 14 and 16 were encoded into a Levenburg-Marquardt algorithm and used to solve for values of K_a, K_b, and P_a/P_b, which appear in Table I. Figs. 2 and 3 display the model calculations simulating experimental assessment of the transport parameters and correspond to Figs. 3 and

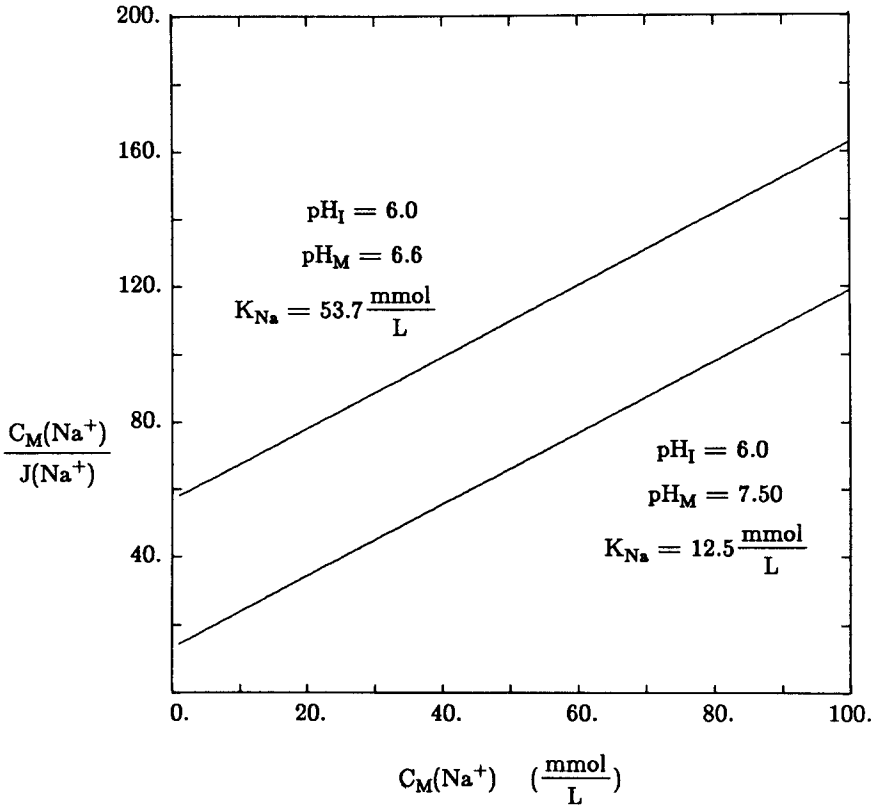

FIGURE 3. Effect of external pH on the Michaelis constant of Na^+ flux. Internal pH 6.0 and internal Na^+ = 0.0 mmol/liter NH_4^+ is absent. Na^+ flux (relative to maximal zero *trans* flux) is computed as a function of external Na^+ at two values of external pH, 6.6 or 7.5. Data are graphed as a Hanes-Woolf plot.

4 of the paper of Aronson et al. (1983). In Fig. 2, the zero *trans* Na^+ influx is computed with external Na^+ = 0.1 mmol/liter for a range of external pH, and this is displayed in the left. Here the flux, $J(Na^+)$, is given as a fraction of maximal flux through the antiporter (i.e., large external Na^+ and acid interior). With reference to Eq. 13, this maximal flux ($\alpha' \beta'' \rightarrow \infty$) is $J_{max} = x_T P_a P_b/(P_a + P_b)$. When replotted (Fig. 2, *right*) with the reciprocal flux as a function of external H^+ concentration, the ratio of intercept to slope yields K_H = 35.2 nmol/liter. Fig. 3 contains Hanes-Woolf

plots of zero *trans* Na^+ flux as a function of external Na^+ concentration. With reference to Eqs. 15 and 16, the ratio of slope to intercept yields K_{Na} = 53.7 mmol/liter at external pH 6.6 and 12.5 mmol/liter at external pH 7.5, as desired. Early vesicle studies comparing Na^+–Na^+ and NH_4^+-Na^+ exchange suggested comparable transport properties for these two species (Kinsella and Aronson, 1981). In Table I, the permeation coefficient for NH_4^+ has been taken equal to that of Na^+ and the equilibrium constant is 90% that of Na^+. With these parameters, NH_4^+ inhibition of zero *trans* Na^+ uptake has been simulated and plotted in Fig. 4 (compare with Fig.

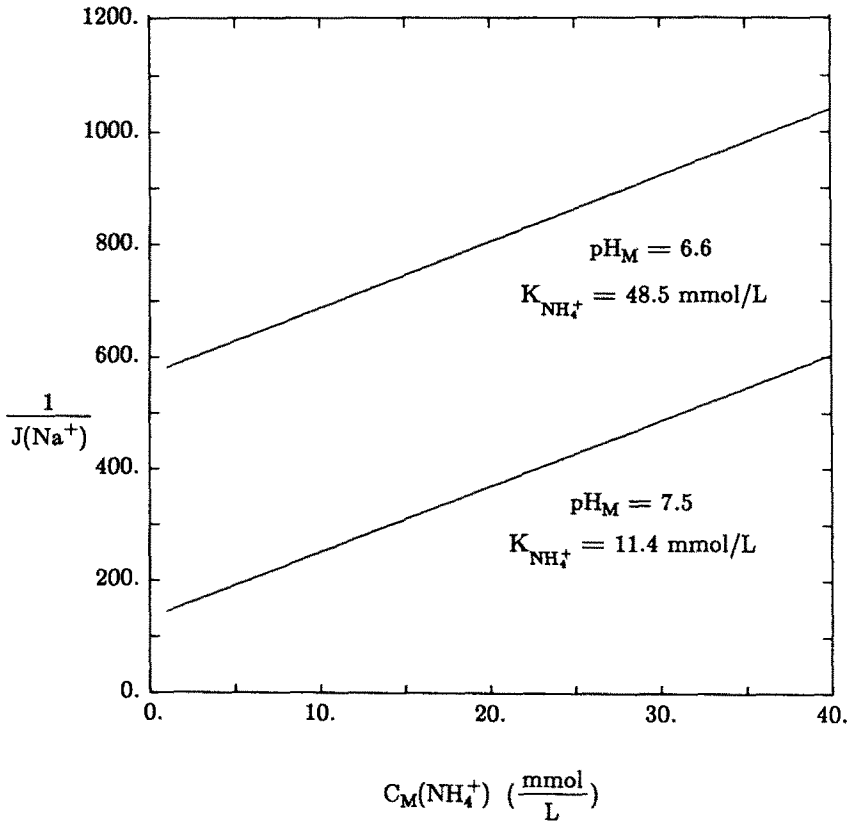

FIGURE 4. Effect of external pH on competitive inhibition by NH_4^+. Internal pH 6.0, internal Na^+ = 0.0 mmol/liter, and external Na^+ = 0.1 mmol/liter. Na^+ flux (relative to maximal zero *trans* flux) is computed as a function of external NH_4^+ at two values of external pH 6.6 or 7.5.

6 in Aronson et al., 1983). At external pH 6.6 the Michaelis constant for NH_4^+, $K_{NH_4^+}$ = 48.5 mmol/liter and at pH 7.5, $K_{NH_4^+}$ = 11.4 mmol/liter. The corresponding values obtained by Aronson et al. (1983) are 50 and 11 mmol/liter.

All of the kinetic parameters thus far have been determined at internal pH 6.0. If these parameters are constant and one computes zero *trans* Na^+ flux as a function of internal pH one obtains a 5% decrease at pH_I = 6.5, 17% decrease at pH_I = 7.0 and a 43% decrease at pH_I = 7.5. This curve is displayed in Fig. 5 (no modifier). These

values may be compared with decreases of 50, 90, and nearly 100% observed by Aronson et al. (1982) and shown in their Fig. 1. The ability to turn off the Na^+/H^+ antiporter with cytosolic alkalinization mandates the sharper dependence on pH_I given by the modifier. Taking a derivative of Eq. 19 reveals that the greatest dependence of P_a on *[H] comes when* $P_a^0 = 0$, and this value has been used in Table I. The Michaelis constant for the modifier is not known with certainty, due in part to difficulties in studying cells below pH_I 6.0. It appears that half-maximal H^+ binding

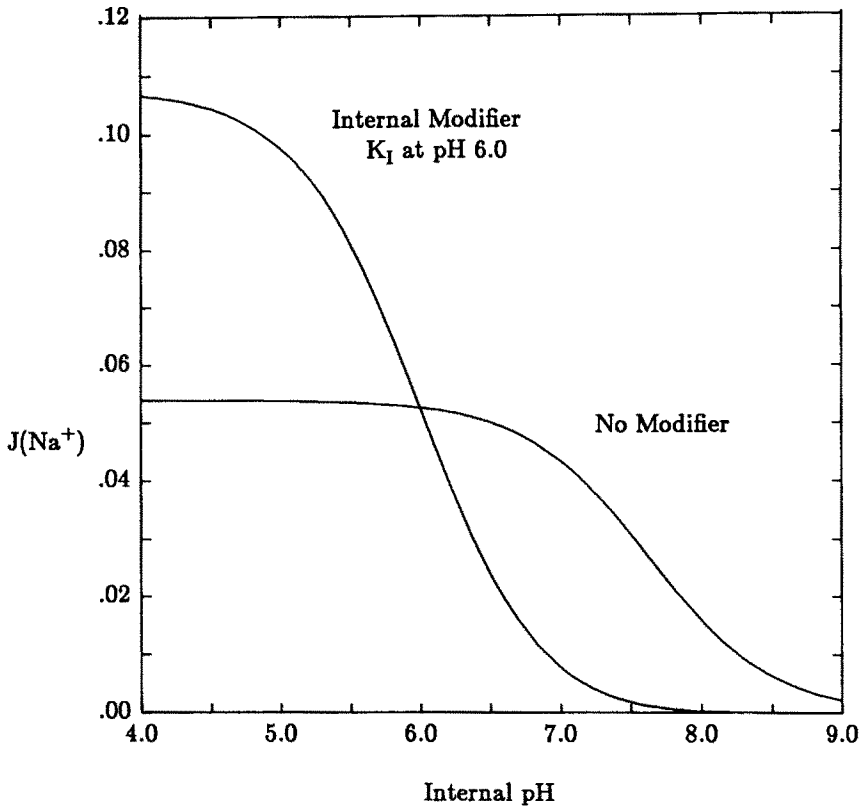

FIGURE 5. Effect of internal pH on Na^+ influx. External Na^+ = 1.0 mmol/liter, external pH 7.26, and internal Na^+ = 0.0 mmol/liter. NH_4^+ is absent. Na^+ flux (relative to maximal zero *trans* flux) is computed as a function of internal pH. The curve labeled *no modifier*, is computed using the permeation velocities of Table I as constants in Eq. 13. For the curve labeled *modifier*, the P_i are computed according to Eq. 19.

occurs at concentrations >0.35 μmol/liter (pH < 6.5, Nord et al., 1986; Kinsella et al., 1986; Orlowski, 1993) and with efforts to examine a broad range of internal pH, greater values for K_y are obtained: 0.63 μmol/liter (pH 6.2, Vigne, Jean, Barbry, Frelin, Fine, and Lazdunski, 1985) and 1.35 μmol/liter (pH 5.9, Restrepo, Cho, and Kron, 1990). A value for K_y toward the high end of the range, 1.0 μmol/liter was selected for model calculations to be able to represent the shut off of Na^+/H^+

exchange with cellular alkalosis. At this value, decreases (from the flux at pH_I 6.0) of 56, 85, and 97% are obtained at pH_I 6.5, 7.0, and 7.5.

One tool which has been used by experimental investigators to discern the cooperative effect of internal H^+ on antiporter turnover has been the Hill plot, namely the plot of log $\{J(Na^+)/[J_{max}(Na^+) - J(Na^+)]\}$ as a function of pH. For the external binding site this slope is 1.0 (Warnock et al., 1982). For internal binding the slope has been reported between 1 and 2 (e.g., 1.2, Kinsella et al., 1986; 1.67, Otsu et

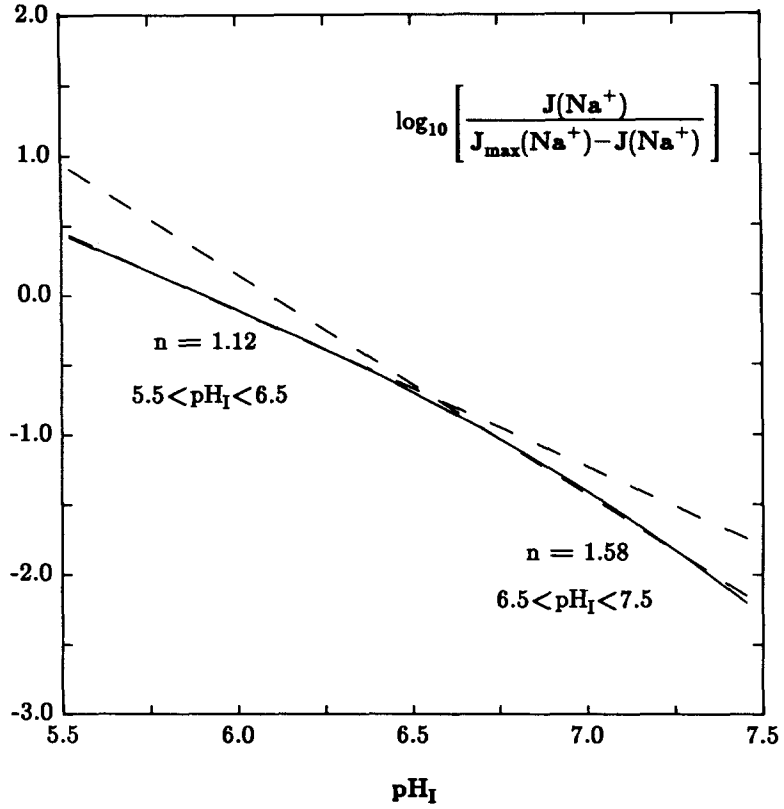

FIGURE 6. Hill plot of Na^+ flux as a function of internal pH. External Na^+ = 140. mmol/liter, external pH 7.50, and internal Na^+ = 20 mmol/liter. NH_4^+ is absent. On the ordinate is $\log_{10}$ $[J(Na^+)/[J_{max}(Na^+) - J(Na^+)]]$. Linear regressions (*dashed lines*) fit to the left and right halves of the Hill curve, with each slope, n, an estimate of the average Hill coefficient for that domain.

al., 1992) and when examined over a broad range of internal pH, the Hill coefficient was found to increase from 1 toward 2 as one proceeded from acid to more neutral pH_I (Restrepo et al., 1990). Fig. 6 displays a Hill plot of the model antiporter as pH_I is varied between 5.5 and 7.5. The dashed lines are linear regressions for the domains $5.5 < pH_I < 6.5$ and $6.5 < pH_I < 7.5$. In the acid domain the Hill coefficient is 1.12 and this increases to 1.58 at more neutral pH. The kinetics imposed by the internal H^+ modifier site also have an impact on NH_4^+ secretion by

the antiporter. In Fig. 7, Na^+, H^+, and NH_4^+ antiporter fluxes are computed for physiologic Na^+ and NH_4^+ concentrations and plotted as a function of cytosolic pH. In the absence of the modifier, increases in cytosolic pH increase the availability of the internal transport site for NH_4^+ binding and thus substantially enhance NH_4^+ secretion. However, with the sharper decline in antiporter turnover imposed by cytosolic alkalinization, NH_4^+ secretion is stabilized over a broad range of internal pH.

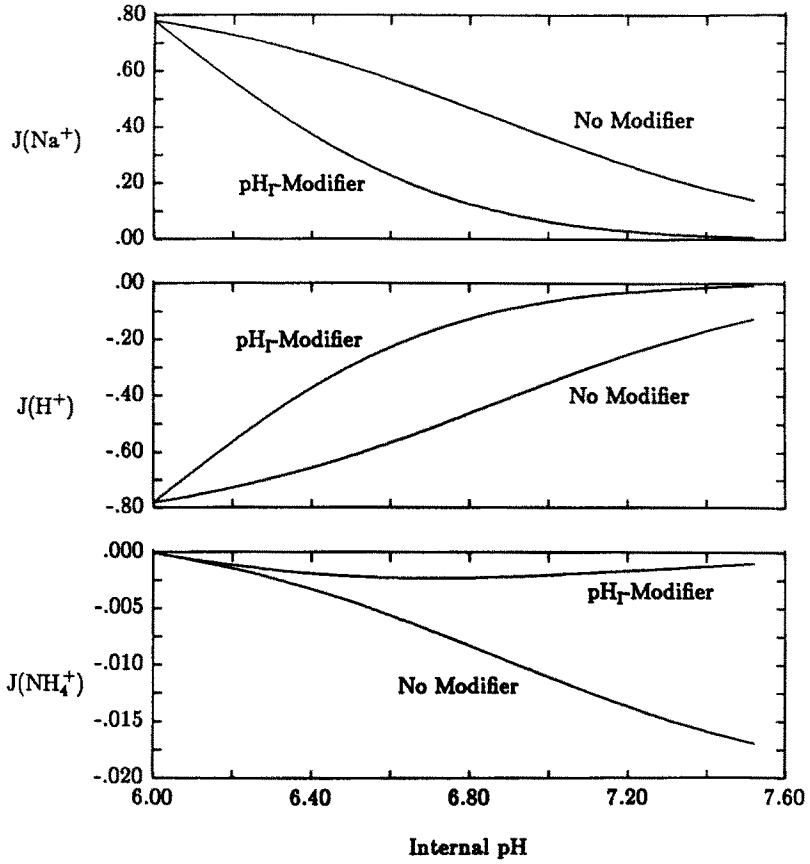

FIGURE 7. Antiporter fluxes as a function internal pH. External Na^+ = 140. mmol/liter, pH 7.30, and NH_4^+ = 0.4 mmol/liter; internal Na^+ = 20 mmol/liter and NH_4^+ = 0.4 mmol/liter. Fluxes of Na^+, H^+, and NH_4^+ are computed with and without the internal modifier, and plotted relative to maximal zero *trans* Na^+ flux. Fluxes from external to internal surface are designated as positive.

The Na^+/H^+ antiporter thus configured was incorporated within a model of the rat proximal tubule which has recently been reported (Weinstein, 1994). This proximal tubule model includes both cellular and paracellular compartments, and represents the fluxes of many of the solute species which are transported by this nephron segment: Na^+, K^+, Cl^-, HCO_3^-, HCO_2^-, $HPO_4^=$, NH_4^+, glucose, and urea. At the luminal cell membrane there is, beyond Na^+/H^+ flux, coupled entry of Na^+ with

glucose and phosphate, and entry of Cl^- in exchange for HCO_3^- and HCO_2^-, there is also a H^+-ATPase. At the peritubular membrane, Na^+ exits via the Na^+, K^+-ATPase, Cl^- exits via KCl cotransport and $Na^+ - 2\ HCO_3^-/Cl^-$exchange, and HCO_3^- exits via Na^+ cotransport (in a 3:1 ratio). With respect to NH_4^+ fluxes, in addition to transport on the Na^+/H^+ exchanger, NH_4^+ can traverse K^+ channels and compete with K^+ for transport on the Na^+, K^+-ATPase. The model also includes a term representing cellular ammoniagenesis. With suitable parameter choices, this model epithelium has

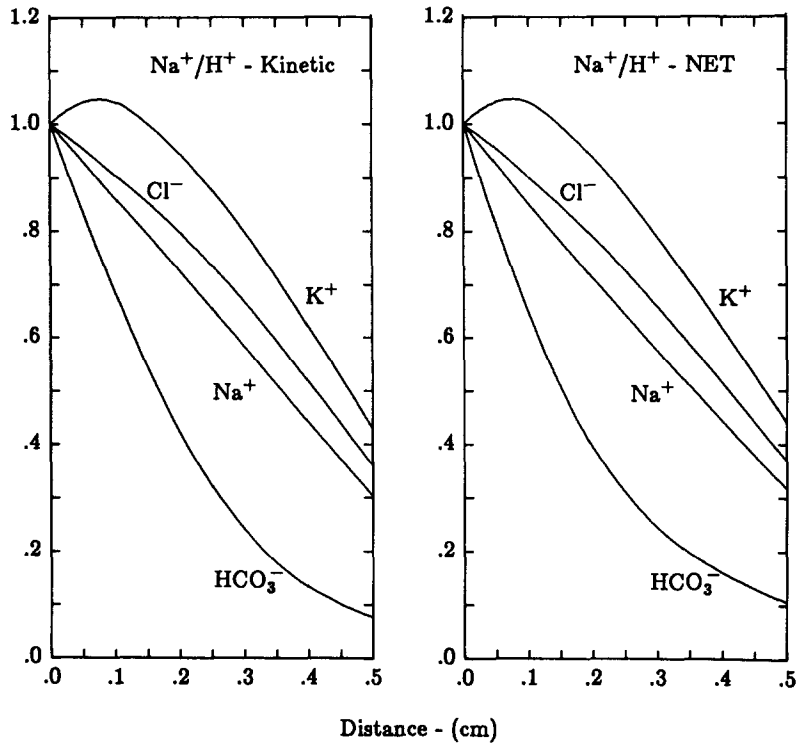

FIGURE 8. Proximal tubule flows of Na^+, K^+, Cl^-, and HCO_3^- relative to initial load, plotted as a function of distance along the tubule. (*Right*) (Na^+/H^+-NET) Calculations from a previously developed proximal tubule model (Weinstein, 1994) in which all coupled transport is represented by linear nonequilibrium thermodynamic formulas. (*Left*) (Na^+/H^+-kinetic) the model is identical, with the exception of replacement of the Na^+/H^+ antiporter by that developed in this work.

permeabilities, solute fluxes, and cytosolic concentrations generally compatible with those obtained for the S2 segment of rat proximal tubule. Up to this point, all coupled transporters of the model were represented by the formalism of linear nonequilibrium thermodynamics (NET), namely with a fixed stoichiometry and a single rate constant.

With all other parameters held constant, the Na^+/H^+ exchanger of this NET model could be replaced by the transporter developed here. The transporter density

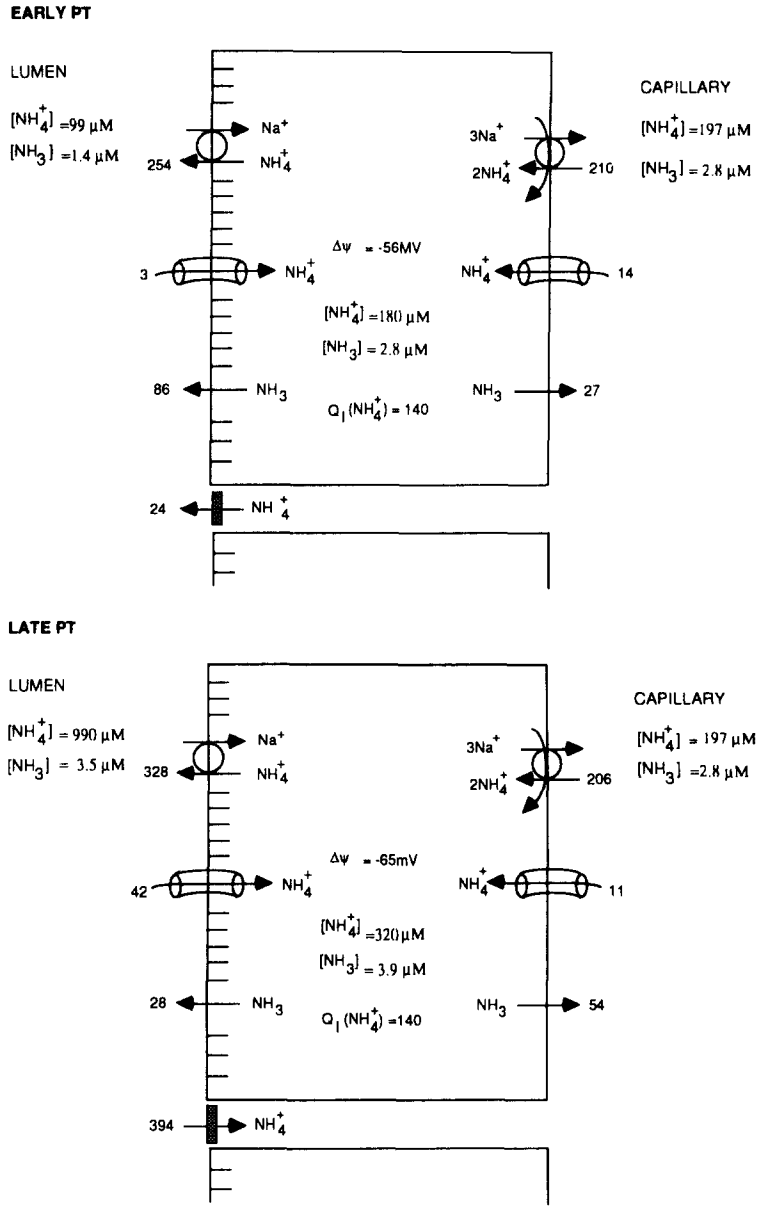

FIGURE 9. Using the proximal tubule model, luminal concentration and epithelial ammonia fluxes are determined along a 0.5–cm segment perfused at 0.5 nl/s. Perfusate ammonia concentration is 100 μmol/liter and bath ammonia concentration is 200 μmol/liter. The epithelial fluxes are depicted at the inlet and outlet of the perfused segment. At the luminal surface are Na^+/NH_4^+ exchange, electrodiffusive flux of NH_4^+ through cell membrane channels, diffusion of NH_3 across cell membranes, and tight junction NH_4^+ flux. At the peritubular surface, transport by the Na^+ pump, channel flux of NH_4^+, and membrane diffusion of NH_3 are shown. Epithelial production of ammonia is $Q_J(NH_4^+)$. Fluxes are in nmol/s.cm^2.

was chosen to yield agreement with respect to overall Na^+ reabsorption along the length of the tubule. In the calculations of Fig. 8, a 5-mm tubule segment is bathed and perfused with standard solutions in which HCO_3^- = 24 mmol/liter, *pCO2* = 50 mm Hg, and the luminal perfusion rate is 0.5 nl/s. The axial flow of Na^+, K^+, Cl^- and HCO_3^- (normalized to initial load) have been plotted as a function of distance

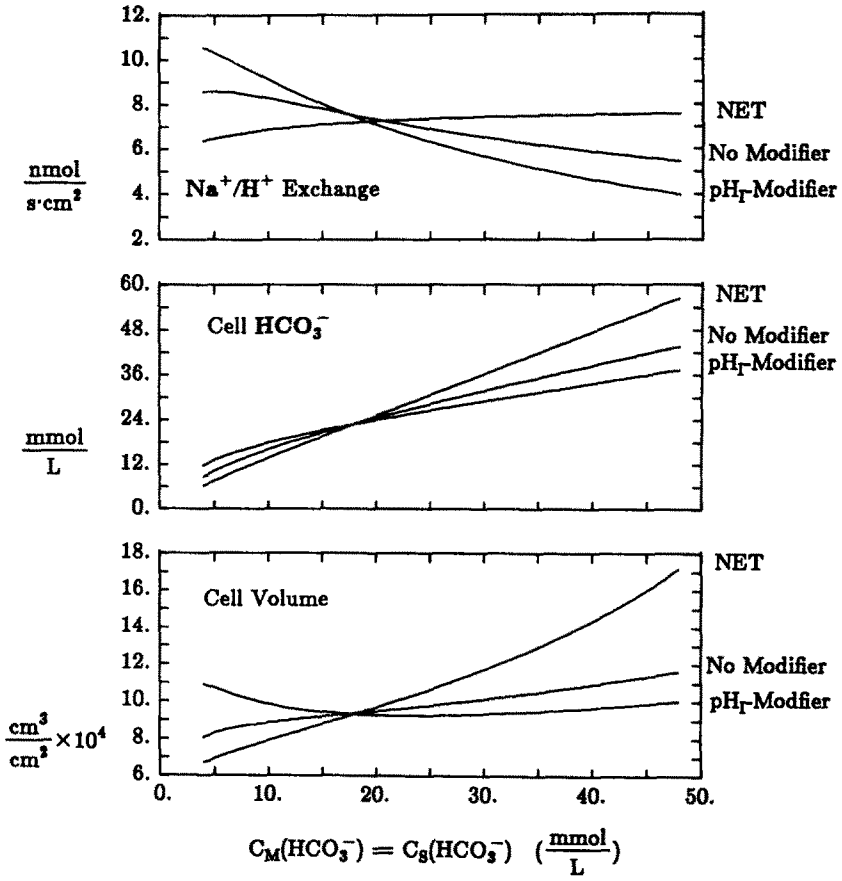

FIGURE 10. Proximal epithelial response to changes in ambient HCO_3. Antiporter Na^+ flux, cell HCO_3 concentration, and cell volume are plotted when both luminal and peritubular HCO_3 concentrations are varied simultaneously. The curves labeled NET are from the previously developed model of proximal tubule epithelium (Weinstein, 1994). For the remaining curves, the Na^+/H^+ antiporter has been replaced by that developed in this work, either with or without the internal modifier site.

along the tubule for the NET model and the model with the kinetic antiporter. For both models, about two thirds of the Na^+ is reabsorbed and ~90% of the HCO_3^-. Fig. 9 displays schematic cells from early and late proximal tubule for the perfusion simulation of Fig. 8 using the kinetic antiporter. In these cells, all of the ammonia

pathways are shown along with the magnitude of the fluxes. With perfusate ammonia concentration 0.1 mmol/liter, and that of the peritubular solution 0.2 mmol/liter, the end proximal ammonia concentration is 1.0 mmol/liter. In the early and late proximal tubule, NH_4^+ flux through the Na^+/H^+ antiporter remains the dominant route for ammonia secretion.

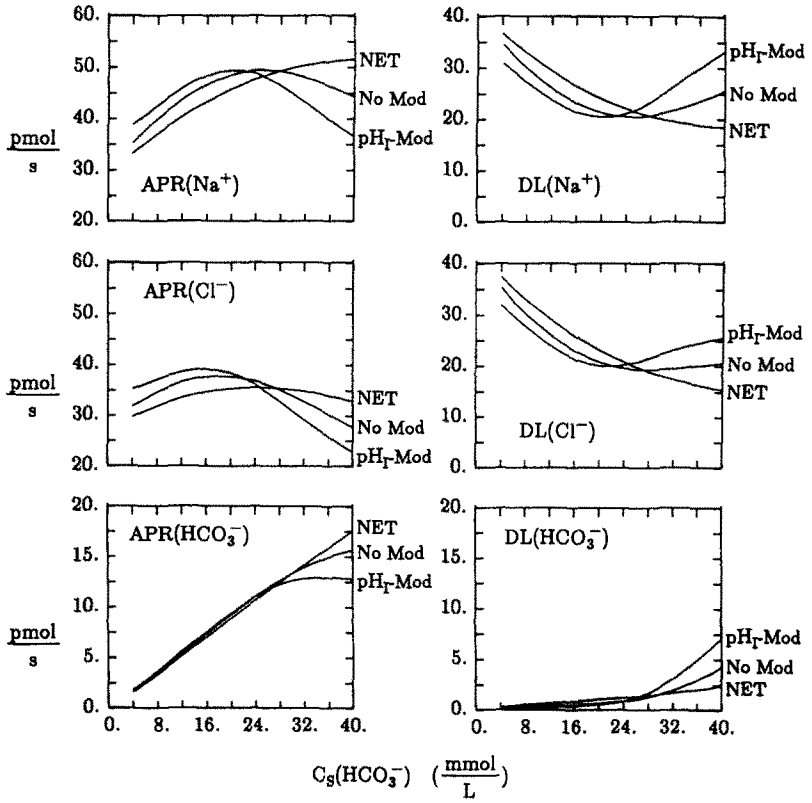

FIGURE 11. Proximal tubule reabsorption of Na^+, Cl^-, and HCO_3 in response to changes in ambient HCO_3. Calculations simulate perfusion of 0.5-cm segment of tubule at 0.5 nl/s using either the NET or kinetic formulation of the Na^+/H^+ antiporter (with or without the internal pH_I modifier). The tubule is perfused and bathed in the same solution, whose HCO_3 concentration is indicated on the abcissa. The left-hand panels show the absolute proximal reabsorption (pmol/s) and those on the right, the end-proximal flow (delivered load).

The impact of ambient HCO_3^- concentration on proximal tubule function is examined in Figs. 10–13. For the calculations of Fig. 10, three epithelial models are used: the model with the kinetically defined Na^+/H^+ antiporter (including the internal modifier), the kinetic model without the internal modifier (see Fig. 5), and the previously developed NET model. In these simulations both luminal and peritubular HCO_3^- concentrations are varied from 4 to 48 mmol/liter, and flux

through the antiporter, cytosolic HCO_3^-, and cell volume are plotted. As shown in the upper panel, the bilateral increase in HCO_3^- has a negligible effect on the electrochemical driving force for H^+ across the antiporter, and thus, a negligible impact on flux in the NET model. In contrast, there is nearly a threefold variation in flux rate when going from alkaline to acid conditions in the full kinetic model. As a consequence of the sensitivity to internal pH, the kinetic model with modifier supplies the cell with a measure of pH homeostasis and volume homeostasis, not seen with the NET model or in the absence of the modifier.

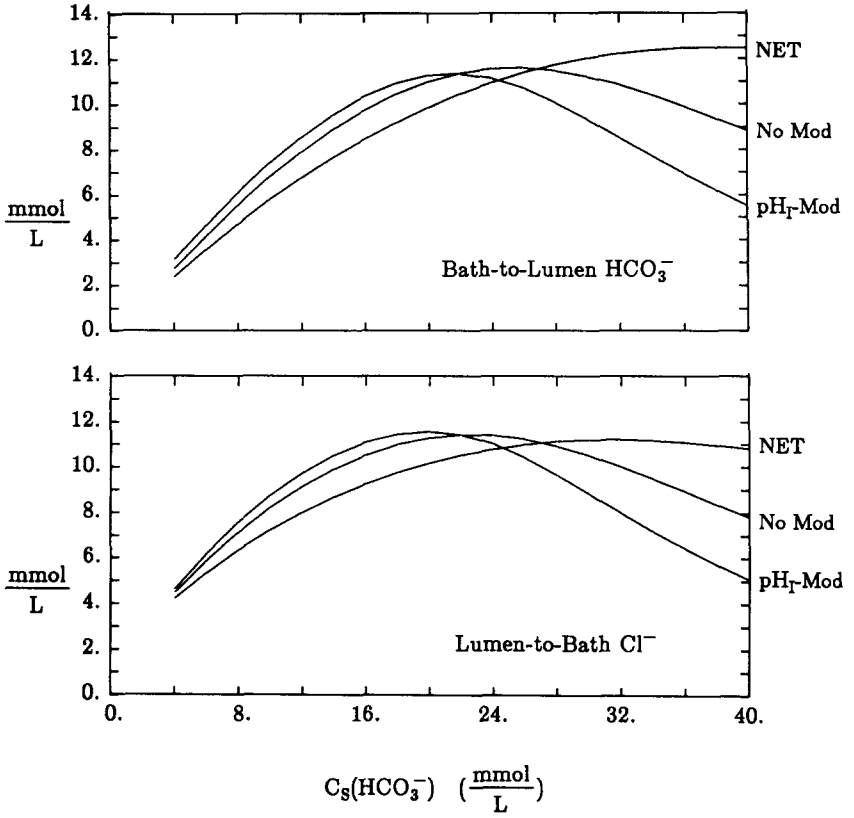

FIGURE 12. Mean transtubular concentration gradients of HCO_3 and Cl^- in response to changes in ambient HCO_3. For the same calculations of Fig. 11, the luminal profiles of Cl^- and HCO_3 have been integrated and subtracted from the concentration in the peritubular solution.

Figs. 11 and 12 compare the kinetic antiporter with the NET model in a tubule simulation in which peritubular and perfusate HCO_3^- is varied from 4 to 40 mmol/liter. Tubules are 5 mm long and perfused at a constant 0.5 nl/s. In Fig. 11 (*left*), the absolute proximal reabsorption (APR) of Na^+, Cl^-, and HCO_3^- are plotted (pmol/s) and on the right the end proximal flows of these species (delivered load,

DL). It is clear that with peritubular alkalinization, proximal HCO_3^- reabsorption by the kinetic model plateaus and there begins to be significant distal delivery. With the internal modifier site in place, this effect is most prominent. What should also be noted is that when peritubular HCO_3^- is 40 mmol/liter and distal delivery of HCO_3^- reaches 7 pmol/s, the distal delivery of Na^+ has increased by nearly twice this

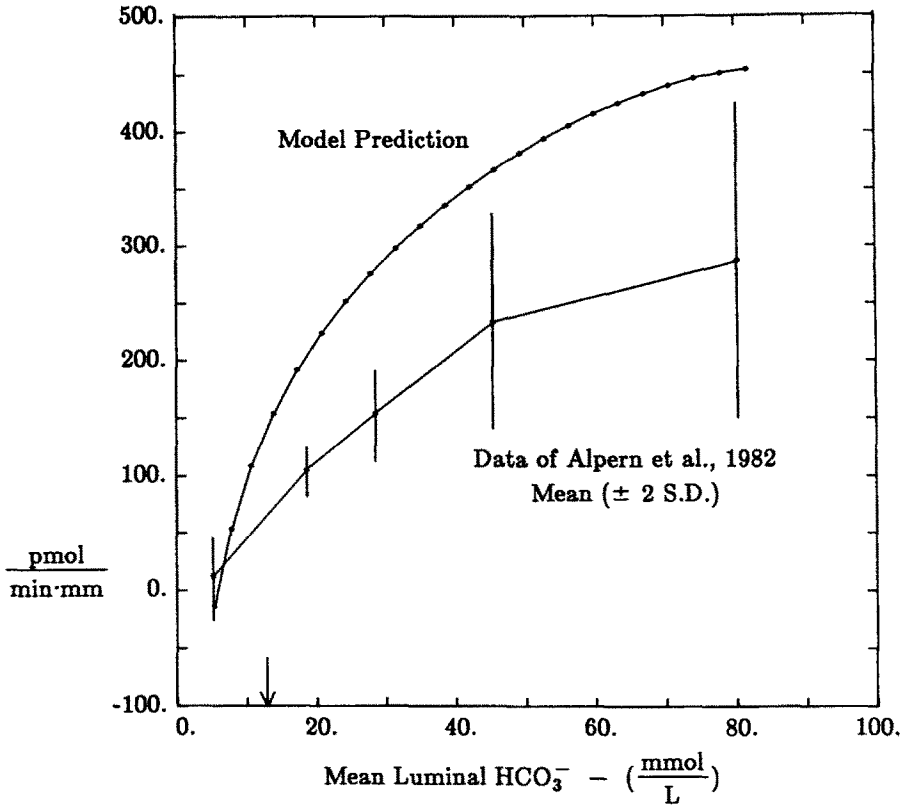

FIGURE 13. Proximal tubule HCO_3 reabsorption as a function of luminal HCO_3. Using the kinetic formulation of the Na^+/H^+ antiporter, calculations simulate perfusion of a 0.5-cm segment of tubule at 2.0 nl/s. Peritubular HCO_3 concentration is 24 mEq/liter, and perfusate HCO_3 concentration is varied. Mean luminal HCO_3 is obtained by numerical integration along the tubule length. The arrow indicates the mean luminal HCO_3 concentration when perfusate HCO_3 is 24 mEq/liter. For comparison, microperfusion data from Alpern et al. (1982) are displayed.

amount. The difference, obviously, is made up by increased distal delivery of Cl^-, and the decrease in APR (Cl^-) derives almost entirely from decreased paracellular reabsorption of Cl^-. Fig. 12 indicates the forces responsible for this decrease. The curves in this figure were obtained by numerical integration and averaging of the luminal concentrations of Cl^- and HCO_3^- and plotting them as a function of the perfusate (and bath) concentration of HCO_3^-. Under all conditions, a lumen to bath

Cl^- concentration gradient develops which is approximately equal in magnitude to the oppositely directed HCO_3^- gradient. This Cl^- gradient is not only responsible for diffusive reabsorption of Cl^- but also for convective paracellular Cl^- reabsorption (via differences in Cl^- and HCO_3^- reflection coefficients). With the decrease in Na^+/H^+ exchange under cellular alkalosis, the magnitude of the mean transepithelial gradients declines and results in decreased paracellular fluxes. This feature was not seen in the NET model, and it may be considered a salutary feature of the antiporter kinetics that enhanced delivery of Na^+, Cl^-, and HCO_3^- would be available for the distal nephron to mediate recovery from metabolic alkalosis.

The plateau of HCO_3^- reabsorption in Fig. 11, ~12.5 pmol/s or 150 pmol/min · mm, must be understood in light of the bilateral (luminal and peritubular) application of HCO_3^- in these simulations. When only luminal HCO_3^- is increased, the reabsorptive capacity of this model tubule is substantially greater, as illustrated in Fig. 13. Here the tubule is perfused at 2.0 nl/s with solutions in which the HCO_3^- concentration varies from 4.0 to 92.0 mEq/l, and peritubular HCO_3^- is fixed at 24.0 mEq/liter. In the figure, proximal HCO_3^- reabsorption is plotted as a function of mean luminal HCO_3^- concentration (obtained by numerical integration along the tubule length). The arrow indicates the point at which perfusate HCO_3^- is 24.0 mEq/liter. One sees here that in the absence of concomitant peritubular alkalinization, HCO_3^- reabsorption by this model tubule may reach 450 pmol/min.mm. For comparison, the experimental microperfusion data of Alpern, Cogan, and Rector (1982) have been plotted in Fig. 13. Comparison of the model prediction with experimental data suggests curves of similar shape (comparable affinity) but with a slightly greater capacity of the model tubule. This may reflect the choice of tubule parameters to fashion a tubule which could represent total proximal reabsorption at 5 mm.

DISCUSSION

A kinetic model of the luminal membrane Na^+/H^+ antiporter has been incorporated within a mathematical model of the rat proximal tubule (Weinstein, 1994). In the original model, all of the coupled transporters were specified by linear nonequilibrium thermodynamic formalism, i.e., by a fixed stoichiometry and a single rate coefficient. The present model provides the opportunity to select affinity and permeation coefficients for each solute plus an affinity for the internal H^+ modifier site; five parameters in all for Na^+/H^+ exchange, or seven parameters to include NH_4^+ transport. Still, the present approach is by no means the most general (Heinz, 1978; Turner, 1983; Stein, 1986; Andersen, 1989). The principal simplifying assumptions made in this approach are that ion binding is rapid relative to translocation, and that both binding and translocation are symmetric (with respect to outer and inner membrane faces). This reduces the requirement for selection of rate constants for binding (and/or occlusion) and unbinding to choice of a single equilibrium constant. It also reduces determination of forward and reverse translocation velocities to assignment of a single permeation coefficient. The more general approach has been taken by Otsu, Kinsella, Heller, and Froehlich (1993) in their examination of kinetic transients of the Na^+/H^+ antiporter. Unfortunately, their model is not suitable for direct incorporation here because (*a*) it is restricted to one

half of the transport cycle (Na^+ uptake) and (*b*) the coefficients were determined at 0°C. The other simplifying assumptions, namely, no slippage (1:1 stoichiometry) and sequential transport of Na^+ and H^+ appear to be justified by experimental studies of the antiporter (Otsu et al., 1992).

The antiporter of this work was adapted from the approach of Heinz (1978) with the inclusion of competitive NH_4^+ transport. At internal pH 6.0, all model parameters could be obtained from the data of Aronson et al. (1983). With these parameters, however, the antiporter would be predicted to be active well above internal pH 8.0, whereas the observations of Aronson et al. (1982) specified a much sharper cutoff. Inclusion of an internal modifier site yielded acceptable flux curves with a pK 6.0, within the range of reported values. With respect to the modifier site, at least two options were available for representing the effect of internal pH to enhance transport. The option selected here was an effect on the rate of (all) ion translocation. (Because H^+ translocation is rate limiting the translocation effect could have been restricted to this species.) Supporting this approach, Otsu et al. (1989) determined an increase in the turnover number for Na^+ transport with internal acidification. The effect could be thought of as an overall decrease in the activation energy for conformational changes of the loaded transporter. Alternatively, the second option for the modifier could be to decrease the equilibrium binding constant for H^+ of the transport site (K_b). In calculations not shown, increases in H^+ affinity of the transport site can mediate nearly proportional increases in Na^+/H^+ flux. However, at present there appear to be no experimental investigations which address the plausibility of such a model. Additional studies into the kinetic sequellae of H^+ binding to the modifier may be motivated by the importance of this site as a target point for hormonal control of Na^+/H^+ exchange (Moolenaar, Tsien, van der Saag, and Laat, 1983; Paris and Pouyssegur, 1984; Miller and Pollack, 1987).

The motivation of the present work has been to identify an acceptable, albeit approximate model of the Na^+/H^+ antiporter and examine it in the context of the other transport pathways of proximal tubule. There have been two previous models of proximal tubule which have included a kinetic antiporter. The first was that of Verkman and Alpern (1987) in which the important pathways for Na^+, H^+, and HCO_3^- were included. That model was used to examine transient changes in the cell in response to perturbations in the bathing media. Their model of the antiporter, however, was empirical and not derived from a specific set of kinetic equations. In particular, their model equation (Eq. 3) shows a Na^+ flux that is quadratic in the internal H^+ concentration, and therefore not a saturable function. The cellular model also did not represent luminal membrane Cl^- flux, so that antiporter turnover was limited to HCO_3^- reabsorption. More recently, a comprehensive model of rat proximal tubule has been presented by Thomas and Dagher (1994). The focus of their investigation was the apparent flow-related increase in proximal Na^+/H^+ exchange. They observed that in situations in which luminal concentration of HCO_3^- tended toward equilibrium, flow dependence would be a property of the whole tubule, but not of the individual transporter. Their model of the Na^+/H^+ antiporter was again empirical, and their antiporter equation (Eq. 6) fails to go to zero in the presence of equal and opposite chemical potential gradients for Na^+ and H^+.

Of note, the graph of antiporter flux as a function of internal pH (Fig. 5) appears

quite linear over a broad range (pH_I 5.0 to 7.0). This linearity has been a general finding in a variety of systems in which Na^+/H^+ has been examined as a function of pH_I (Grinstein, Cohen, and Rothstein, 1984; Boyarsky, Ganz, Cragoe, and Boron, 1990; Sjaastad, Wenzl, and Machen, 1992; Watson, Levine, Donowitz, and Montrose, 1991). Its presence provides some measure for the range of applicability of linear nonequilibrium thermodynamic models of the epithelial cell. Indeed, with respect to overall transport properties, the NET model of proximal tubule and the model of this paper could be brought into good agreement (Fig. 8). Nevertheless, certain kinetic properties of the Na^+/H^+ exchanger were clearly salutary for cellular homeostasis. In its initial description, Aronson et al. (1982) suggested the importance of the internal modifier as a defense against intracellular acidosis. The calculations shown here also illustrate the utility of this feature as a powerful defense against cell volume increase in metabolic alkalosis (Fig. 10). Further, by blunting proximal reabsorption of Na^+, HCO_3^-, and Cl^-, decreases in flux through this antiporter would also be expected to be helpful in recovery from metabolic alkalosis.

Micropuncture of the rat proximal tubule during systemic infusion of bicarbonate (acute metabolic alkalosis) has indicated that as filtered HCO_3^- increases above normal, the absolute proximal reabsorption of HCO_3^- remains relatively constant (Cogan and Liu, 1983; Maddox and Gennari, 1986). This observation is reproduced in the calculations of Fig. 11 here. It was also found that when continuous microperfusion of proximal tubules is used to maintain a constant filtered load, acute metabolic alkalosis depresses proximal tubule proton secretion (Alpern, Cogan, and Rector, 1983), a finding compatible with the fluxes of Fig. 10. With respect to Cl^- transport, the impact of acute alkalosis to decrease absolute proximal NaCl transport (Fig. 11) is suggested by the data of Cogan and Liu (1983), but this aspect of alkalosis has not received extensive examination. Further, this experimental issue is complicated by the independent effect of volume expansion to depress NaCl reabsorption (Cogan, 1983). The situation in chronic metabolic alkalosis is quite different, where even with a doubling of filtered HCO_3^- load above normal, a constant proportion of proximal HCO_3^- is reabsorbed (Maddox and Gennari, 1986). In this regard, the model calculations presented here suggest, that in chronic metabolic alkalosis, the kinetic parameters of the Na^+/H^+ exchanger must be altered. One might anticipate an increase in the Vmax of the Na^+/H^+ exchanger, akin to that seen when a change in GFR is used to increase the filtered load of HCO_3^- (Maddox, Fortin, Tartini, Barnes, and Gennari, 1992). Finally, in studies of renal HCO_3^- reabsorption, the concept of a transport maximum, $Tm(HCO_3^-)$ has been introduced to quantify the capacity of this system. As illustrated in the calculations here (Figs. 11 and 13), the Tm could apply to either acute alkalosis or to a unilateral luminal load, but would be very different for each, and both would be different from the nephron Tm defined in whole organ experiments.

Previous analysis of ammonia transport (Weinstein, 1994) indicated that luminal membrane Na^+/NH_4^+ exchange, cellular production of ammonia, and peritubular membrane NH_4^+ uptake (via Na^+, K^+ ATPase or via K^+ channel) all act in parallel to drive ammonia secretion. This derives from the cellular interconversion of NH_4^+ and NH_3, and the free permeation of NH_3 across cell membranes. It implies that inhibition of the luminal membrane transporter does not block the contribution of

peritubular uptake or ammoniagenesis to the overall active transport of ammonia. In that model, an estimate for ammonia transport on the Na^+, K^+ ATPase could be obtained from the overall rate of Na^+ transport and the known affinity of NH_4^+ and K^+. Given the measured rate for ammoniagenesis, it was calculated that the concentrations of luminal ammonia observed in late proximal tubule could not be achieved without substantial NH_4^+ secretion by the Na^+/H^+ exchanger. The calculations of this model, based on the kinetics of the exchanger, thus confirm the prediction of a substantial role for the Na^+/H^+ antiporter in the secretory flux of ammonia. The fluxes are not quite as large as had been estimated using the NET model, but among the three forces for active ammonia secretion (Na^+/H^+ antiporter, Na^+, K^+ ATPase and ammoniagenesis) it appears to be most important.

The selection of the Na^+/H^+ antiporter was a logical first choice for amplification of this proximal tubule model. It is the most important pathway in proximal Na^+ reabsorption, and this transporter has been perhaps the most intensively investigated. With the relatively recent cloning of NHE-3, one may anticipate additional kinetic information to accrue. As indicated above, the identification of the kinetic effect of the modifier site is a natural focus of inquiry. A second focus might be the kinetic basis for enhancement of antiporter flux with axial flow. Gennari, Helmle-Kolb, and Murer (1992) observed an increase in antiporter flux in QK cells when superfusion rates were increased, and they could discern no gross change in Na^+ affinity, K_{Na}. With reference to Eq. 16, this could be accomplished by parallel increases in all translocation velocities or else an overall increase in antiporter density. Beyond the Na^+/H^+ antiporter, it is clear that reconstruction of a proximal tubule model with kinetically defined transporters will be costly. At present, it appears that only a sodium-dependent glucose cotransporter has been characterized sufficiently well to be included in such a model (Parent, Supplisson, Loo, and Wright, 1992). Nevertheless, such an undertaking appears to be the only means of discerning the quantitative impact of the modulation of transport kinetics on overall tubule function.

The author gratefully acknowledges valuable discussions with Dr. Olaf S. Andersen.

This investigation was supported by United States Public Health Services Grant 1-R01-DK-29857 from the National Institute of Arthritis, Diabetes, and Digestive and Kidney Disease. A.M. Weinstein is the recipient of an Irma T. Hirschl Career Scientist Award.

Original version received 17 October 1994 and accepted version received 9 January 1995.

REFERENCES

Alpern, R. J., M. G. Cogan, and F. C. Rector, Jr. 1982. Effect of luminal bicarbonate concentration on proximal acidification in the rat. *American Journal of Physiology*. 243:F53–F59.

Alpern, R. J., M. G. Cogan, and F. C. Rector, Jr. 1983. Effects of extracellular fluid volume and plasma bicarbonate concentration on proximal acidification in the rat. *Journal of Clinical Investigation*. 71:736–746.

Alpern, R. J., M. G. Cogan, and F. C. Rector, Jr. 1983. Flow dependence of proximal tubular bicarbonate absorption. *American Journal of Physiology*. 245:F478–F484.

Andersen, O. S. 1989. Kinetics of ion movement mediated by carriers and channels. *In* Methods in Enzymology. Part R. Transport Theory: Cells and Model Membranes.Vol. 171. Biomembranes. S. Fleischer and B. Fleischer, editors. Academic Press, NY. 62–112.

Aronson, P. S. 1985. Kinetic properties of the plasma membrane Na^+-H^+ exchanger. *Annual Review of Physiology.* 47: 545–60.

Aronson, P. S., J. Nee, and M. A. Suhm. 1982. Modifier role of internal H^+ in activating the Na^+-H^+ exchanger in renal microvillus membrane vesicles. *Nature.* 299:161–163.

Aronson, P. S., M. A. Suhm, and J. Nee. 1983. Interaction of external H^+ with the Na^+-H^+ exchanger in renal microvillus membrane vesicles. *Journal of Biological Chemistry.* 258:6767–6771.

Bello-Reuss, E. 1980. Effect of catecholamines on fluid reabsorption by the isolated proximal convoluted tubule. *American Journal of Physiology.* 238:F347–F352.

Biemesderfer, D., J. Pizzonia, A. Abu-Alfa, M. Exner, R. Reilly, P. Igarashi, and P. S. Aronson. 1993. NHE3: a Na^+/H^+ exchanger isoform of renal brush border. *American Journal of Physiology.* 265:F736–F742.

Boyarsky, G., M. B. Ganz, E. J. Cragoe, and W. F. Boron. 1990. Intracellular-pH dependence of Na-H exchange and acid loading in quiescent and arginine vasopressin-activated mesangial cells. *Proceedings of the National Academy of Sciences, USA.* 87:5921–5924.

Chan, Y. L., B. Biagi, and G. Giebisch. 1982. Control mechanisms of bicarbonate transport across the rat proximal convoluted tubule. *American Journal of Physiology.* 242:F532-F543.

Cogan, M.G. 1990. Angiotensin II: a powerful controller of sodium transport in the early proximal tubule. *Hypertension.* 15:451–458.

Cogan, M. G. 1983. Volume expansion predominantly inhibits proximal reabsorption of NaCl rather than $NaHCO_3$. *American Journal of Physiology.* 245:F272–F275.

Cogan, M. G., and F. Y. Liu. 1983. Metabolic alkalosis in the rat. Evidence that reduced glomerular filtration rather than enhanced tubular bicarbonate reabsorption is responsible for maintaining the alkalotic state. *Journal of Clinical Investigation.* 71:1141–1160.

Felder, C. C., T. Campbell, F. Albrecht, and P. A. Jose. 1990. Dopamine inhibits Na^+-H^+ exchanger activity in renal BBMV by stimulation of adenylate cyclase. *American Journal of Physiology.* 259:F297–F303.

Gennari, F. J., C. Helmle-Kolb, and H. Murer. 1992. Influence of extracellular pH and perfusion rate on Na^+/H^+ exchange in cultured opposum kidney cells. *Pflügers Archiv.* 420:153–158.

Grinstein, S., S. Cohen, and A. Rothstein. 1984. Cytoplasmic pH regulation in thymic lymphocytes by an amiloride-sensitive Na^+/H^+ antiport. *Journal of General Physiology.* 83:341–369.

Grinstein, S., and A. Rothstein. 1986. Mechanisms of regulation of the Na^+/H^+ exchanger. *Journal of Membrane Biology.* 90:1–12.

Harris, P. J., and L. G. Navar. 1985. Tubular transport responses to angiotensin. *American Journal of Physiology.* 248:F621–F630.

Heinz, E. 1978. Mechanics and Energetics of Biological Transport. Springer-Verlag, Berlin.

Kinsella, J. L., and P. S. Aronson. 1980. Properties of the Na^+-H^+ exchanger in renal microvillus membrane vesicles. *American Journal of Physiology.* 238:F461–F469.

Kinsella, J. L., and P. S. Aronson. 1981. Interaction of NH_4^+ and Li^+ with the renal microvillus membrane Na^+-H^+ exchanger. *American Journal of Physiology.* 241: C220–C226.

Kinsella, J. L., and P. S. Aronson. 1982. Determination of the coupling ratio for Na^+-H^+ exchange in renal microvillus membrane vesicles. *Biochimica et Biophysica Acta.* 689:161–164.

Kinsella, J. L., T. Cujdik, and B. Sacktor. 1986. Kinetic studies on the stimulation of Na^+-H^+ exchange activity in renal brush border membranes isolated from thyroid hormone-treated rats. *Journal of Membrane Biology.* 91:183–191.

Liu, F.-Y., and M. G. Cogan. 1988. Angiotensin II stimulation of hydrogen ion secretion in the rat early proximal tubule. Modes of action, mechanism, and kinetics. *Journal of Clinical Investigation.* 82:601–607.

Lucci, M. S., and D. G. Warnock. 1979. Effects of anion-transport inhibitors on NaCl reabsorption in the rat superficial proximal convoluted tubule. *Journal of Clinical Investigation.* 64:570–579.

Maddox, D. A., S. M. Fortin, A. Tartini, W. D. Barnes, and F. J. Gennari. 1992. Effect of acute changes in glomerular filtration rate on Na^+/H^+ exchange in rat renal cortex. *Journal of Clinical Investigation.* 89:1296–1303.

Maddox, D. A., and F. J. Gennari. 1986. Load dependence of proximal tubular bicarbonate reabsorption in chronic metabolic alkalosis in the rat. *Journal of Clinical Investigation.* 77:709–716.

Miller, R. T., and A. S. Pollock. 1987. Modification of the internal pH sensitivity of the Na^+/H^+ antiporter by parathyroid hormone in a cultured renal cell line. *Journal of Biological Chemistry.* 262: 9115–9120.

Montrose, M. H., and H. Murer. 1988. Kinetics of Na^+/H^+ exchange. *In* Na^+/H^+ Exchange. S. Grinstein, editor. CRC Press, Boca Raton, FL. 57–75.

Moolenaar, W. H., R. Y. Tsien, P. T. van der Saag, and S. W. de Laat. 1983. Na^+/H^+ exchange and cytoplasmic pH in the action of growth factors in human fibroblasts. *Nature.* 304:645–648.

Murer, H., U. Hopfer, and R. Kinne. 1976. Sodium/proton antiport in brush-border-membrane vesicles isolated from rat small intestine and kidney. *Biochemical Journal.* 154:597–604.

Nord, E. P., D. Goldfarb, N. Mikhail, P. Moradeshagi, A. Hafezi, S. Vaystub, E. J. Cragoe, and L. G. Fine. 1986. Characteristics of the Na^+-H^+ antiporter in the intact renal proximal tubular cell. *American Journal of Physiology.* 250: F539–F550.

Orlowski, J. 1993. Heterologous expression and functional properties of amiloride high affinity (NHE-1) and low affinity (NHE-3) isoforms of the rat Na/H exchanger. *Journal of Biological Chemistry.* 268:16369–16377.

Orlowski, J., R. A Kandasamy, and G. E. Shull. 1992. Molecular cloning of putative members of the Na/H exchanger gene family. cDNA cloning, deduced amino acid sequence, and mRNA tissue expression of the rat Na/H exchanger NHE-1 and two structurally related proteins. *Journal of Biological Chemistry.* 267:9331–9339.

Otsu, K., J. L. Kinsella, P. Heller, and J. P. Froehlich. 1993. Sodium dependence of the Na^+-H^+ exchanger in the pre-steady state. Implications for the exchange mechanism. *Journal of Biological Chemistry.* 268:3184–3193.

Otsu, K., J. L. Kinsella, E. Koh, and J. P. Froehlich. 1992. Proton dependence of the partial reactions of the sodium-proton exchanger in renal brush border membranes. *Journal of Biological Chemistry.* 267:8089–8096.

Otsu, K., J. L. Kinsella, B. Sacktor, and J. P. Froehlich. 1989. Transient state kinetic evidence for an oligomer in the mechanism of Na^+-H^+ exchange. *Proceedings of the National Academy of Sciences, USA.* 86:4818–4822.

Parent, L., S. Supplisson, D. D. F. Loo, and E. M. Wright. 1992. Electrogenic properties of the cloned Na^+ glucose cotransporter: II. A transport model under nonrapid equilibrium conditions. *Journal of Membrane Biology.* 125: 63–79.

Paris, S., and J. Pouyssegur. 1984. Growth factors activate the Na^+/H^+ antiporter in quiescent fibroblasts by increasing its affinity for intracellular H^+. *Journal of Biological Chemistry.* 259:10989–10994.

Preisig, P. A. 1992. Luminal flow rate regulates proximal tubule H-HCO_3 transporters. *American Journal of Physiology.* 262:F47–F54.

Preisig, P. A., and F. C. Rector, Jr. 1988. Role of Na^+-H^+ antiport in rat proximal tubule NaCl absorption. *American Journal of Physiology.* 255:F461–F465.

Restrepo, D., D. S. Cho, and M. J. Kron. 1990. Essential activation of Na^+-H^+ exchange by $[H^+]_i$ in HL-60 cells. *American Journal of Physiology*. 259:C490–C502.

Sanders, D., U.-P. Hansen, D. Gradmann, and C. L. Slayman. 1984. Generalized kinetic analysis of ion-driven cotransport systems: a unified interpretation of selective ionic effects on Michaelis parameters. *Journal of Membrane Biology*. 77:123–152.

Sjaastad, M. D., E. Wenzl, and T. E. Machen. 1992. pH_i dependence of Na-H exchange and H delivery in IEC-6 cells. *American Journal of Physiology*. 262:C164–C170.

Thomas, S.R., and G. Dagher. 1994. A kinetic model of rat proximal tubule transport-load-dependent bicarbonate reabsorption along the tubule. *Bulletin of Mathematical Biology*. 56:431–458.

Tse, C.-M., S. R. Brant, M. S. Walker, J. Pouyssegur, and M. Donowitz. 1992. Cloning and sequencing of a rabbit cDNA encoding an intestinal and kidney-specific Na^+/H^+ exchanger isoform (NHE-3). *Journal of Biological Chemistry*. 267:9340–9346.

Tse, C.-M., S. A. Levine, C. H. C. Yun, S. R. Brant, J. Pouyssegur, M. H. Montrose, and M. Donowitz. 1993. Functional characteristics of a cloned epithelial Na^+-H^+ exchanger (NHE3): resistance to amiloride and inhibition by protein kinase C. *Proceedings of the National Academy of Sciences, USA*. 90:9110–9114.

Turner, R. J. 1983. Quantitative studies of cotransport systems: models and vesicles. *Journal of Membrane Biology*. 76:1–15.

Verkman, A. S., and R. J. Alpern. 1987. Kinetic transport model for cellular regulation of pH and solute concentration in the renal proximal tubule. *Biophysical Journal*. 51:533–546.

Vigne, P., T. Jean, P. Barbry, C. Frelin, L. G. Fine, and M. Lazdunski. 1985. [^{3}H] Ethylpropylamiloride, a ligand to analyze the properties of the Na^+/H^+ exchange system in the membranes of normal and hypertrophied kidneys. *Journal of Biological Chemistry*. 260:14120–14125.

Warnock, D. G., W. W. Reenstra, and V. J. Yee. 1982. Na^+/H^+ antiporter of brush border vesicles: studies with acridine orange uptake. *American Journal of Physiology*. 242:F733–F739.

Watson, A. J. M., S. Levine, M. Donowitz, and M. H. Montrose. 1991. Kinetics and regulation of a polarized Na^+-H^+ exchanger from Caco-2 cells, a human intestinal cell line. *American Journal of Physiology*. 261:G229–G238.

Weinman, E. J., S. C. Sansom, T. F. Knight, and H. O. Senekjian. 1982. Alpha and beta adrenergic agonists stimulate water absorption in the rat proximal tubule. *Journal of Membrane Biology*. 69:107–111.

Weinstein, A. M. 1994. Ammonia transport in mathematical model of the rat proximal tubule. *American Journal of Physiology*. 267:F237–F248.